

# Isothermal Piston Skirts EHL Using Viscous Oil at Idling Speed Engine Start Up - Small Radial Clearance Effects

Syed Adnan Qasim, M. Afzaal Malik.

**Abstract**— Adhesive wear of piston skirts and liner occurs at very low engine idling speed in a few initial engine start up cycles. It happens in the absence of a fully developed elastohydrodynamic lubricating (EHL) film and non-optimized small piston-to-bore radial clearance. A 2-D numerical piston skirts hydrodynamic and EHL model is developed and simulated at an idling speed. The simulation results are investigated and analyzed for a range of small piston-to-bore radial clearances. A high viscosity-grade Newtonian engine lubricant is characterized in the model under the isothermal conditions. Such conditions imply an ideal engine heat removal mechanism in the initial engine start up conditions. 2-D Reynolds equation is coupled with the secondary piston motion and film thickness equation to generate the hydrodynamic pressures, piston displacements and film thickness profiles as a function of 720 degree crank rotation cycle. The elastic surface deformations are incorporated in the EHL model and an inverse solution technique is employed to generate EHL pressures and film thickness profiles. The simulation results show variations in the secondary piston eccentricities, film thickness profiles and hydrodynamic pressure fields at different radial clearances. The outcomes of the comparative analysis optimize the small piston-to-bore radial clearance to minimize adhesive wear in the initial engine start up at the idling speed.

**Index Terms**— EHL, Isothermal, Idling Speed, Initial Engine Start up.

## I. INTRODUCTION

In an internal combustion engine, the small secondary oscillations of the piston adversely affect its lubrication in a few initial engine start up cycles. The EHL film does not develop between the piston skirts and the liner surfaces in the initial idling engine start up speed [1]. It invites a physical contact and wear of the interacting surfaces at low speeds [2]. An engine lubricant should facilitate cold engine starting at the critical stage of a few initial crank cycles. At the same time it ought to be viscous enough to cushion the secondary piston displacements and prevent start up wear. The non-optimized piston-to-bore radial clearance in the idling speed engine start up provides an extra space for the secondary oscillations of the piston. Such displacements counter the cushioning effect provided by an engine lubricant. A high viscosity-grade engine lubricant and an appropriate piston-to-bore radial clearance at an idling engine speed of say, 800 rpm may facilitate EHL film formation and reduce the engine start up wear [1]. To analyze the effects of a

small piston-to-bore radial clearance on the hydrodynamic and EHL of piston skirts objectively, it may be appropriate to assume a very efficient engine cooling system and isothermal conditions. In the basic numerical model, the radial clearance is taken as 10 microns. The governing equations of piston axial and transverse motion are solved to calculate the secondary eccentric displacements and velocities of piston. Hydrodynamic pressures are determined by solving the 2-D Reynolds equation. In the EHL model, the piezoviscous effects are considered by defining the pressure-viscosity relationship. The effects of the elastic deformation of the interacting surfaces are incorporated to obtain the EHL film and pressure profiles. The hydrodynamic and EHL models are extended to 20, 30 and 40 microns radial clearance, respectively. The simulation results are compared and analyzed to investigate their effects on the secondary displacements, velocities, film thickness profiles and pressures in the hydrodynamic and EHL regimes. To develop the model, the following logical assumptions are taken:

1. Lubricant is Newtonian and incompressible.
2. Thermal effects are neglected.
3. Waviness and roughness effects of the skirts and liner surfaces are neglected.
4. Pressure at the inlet of contact zone is zero.
5. Lubricant flow is laminar and turbulence effects are neglected.
6. Surfaces are oil-flooded at the time of engine start up.

**Table-1** (Input Parameters)

Parameter	Value	Parameter	Value
$m_{pis}$	0.295 kg	$\theta = \theta_1 + \theta_2$	75 degree
$R$	0.0415 m	$l$	0.133 m
$L$	0.0338 m	$\eta$	0.1891 Pa.S.
$m_{pin}$	0.09 kg	$v_1, v_2$	0.3
$R$	0.0418 m	$E_1, E_2$	200 GPa

## II. MATHEMATICAL MODEL

### A. Governing Equations of Piston Motion

The equations of motion of the piston must be defined by incorporating the small secondary displacements in the form of piston eccentricities along the direction perpendicular to the axis of cylinder. For constant crankshaft speed  $\omega$ , the piston position is [2]:

$$Y = \left[ (l+r)^2 - (C_p)^2 \right]^{0.5} - (l^2 - B^2)^{0.5} - r \cos \psi \quad (1)$$

Manuscript received March 21, 2011. This work was sponsored by Syed Adnan Qasim is research associate at NUST College of Electrical and Mechanical Engineering, (email: adnan\_qasim@yahoo.com)

M. Afzaal Malik is Professor and Associate Dean at College of Electrical & Mechanical Engineering, NUST. (, email: drafzaalmalik@yahoo.com)

For constant crankshaft speed  $\omega$ , the piston speed is [10]:

$$U = \dot{Y} = r\omega \sin \Psi + r\omega B \cos \Psi (l^2 - B^2)^{-0.5} \quad (2)$$

$$\text{where } B = C_p + r \sin \Psi \quad (3)$$

Significant piston skirts eccentricities at the top and bottom are calculated by considering piston inertia, hydrodynamic force, hydrodynamic friction force and moments in the form of equations similar to that defined by Zhu et al [2]:

$$\begin{bmatrix} m_{\text{pis}} \left(1 - \frac{a}{L}\right) + m_{\text{pis}} \left(1 - \frac{b}{L}\right) & m_{\text{pis}} \frac{a}{L} + m_{\text{pis}} \frac{b}{L} \\ \frac{I_{\text{pis}}}{L} + m_{\text{pis}} (a - b) \left(1 - \frac{b}{L}\right) & m_{\text{pis}} (a - b) \frac{b}{L} - \frac{I_{\text{pis}}}{L} \end{bmatrix} \begin{bmatrix} \ddot{e}_t \\ \ddot{e}_b \end{bmatrix} = \begin{bmatrix} F + F_s + F_f \tan \phi \\ M + M_s + M_f \end{bmatrix} \quad (4)$$

### B Reynolds Equation and Hydrodynamic Pressure

To calculate the hydrodynamic pressures and forces, the 2-D Reynolds equation is solved. Reynolds equation in dimensional form is [2]:

$$\frac{\partial}{\partial x} \left( h^3 \frac{\partial p}{\partial x} \right) + \frac{\partial}{\partial y} \left( h^3 \frac{\partial p}{\partial y} \right) = 6\eta U \frac{\partial h}{\partial y} \quad (5)$$

Reynolds equation in non-dimensional form is [3]

$$\frac{\partial}{\partial x^*} \left( h^{*3} \frac{\partial p^*}{\partial x^*} \right) + \left( \frac{R}{L} \right)^2 \frac{\partial}{\partial y^*} \left( h^{*3} \frac{\partial p^*}{\partial y^*} \right) = \frac{\partial h^*}{\partial y^*} \quad (6)$$

Boundary conditions for Reynolds equation are [2]:

$$\frac{\partial p}{\partial x} \Big|_{x=0} = \frac{\partial p}{\partial x} \Big|_{x=\pi} = 0 ;$$

$$\begin{aligned} p &= 0 \text{ when } x_1 \leq x \leq x_2 \\ p(x, 0) &= p(x, L) = 0 \end{aligned} \quad (7)$$

### C. Hydrodynamic Forces and Shear Stress

Hydrodynamic pressure and hydrodynamic friction forces are given by [2]:

$$F_h = R \iint p(x, y) \cos x \, dx dy \quad (8)$$

$$F_{fh} = R \iint \tau(x, y) \, dx dy \quad (9)$$

$$F_{fh} = \iint \left( \eta \frac{U}{h} + \frac{h}{2} \frac{dp}{dy} \right) \, dx dy \quad (10)$$

The total normal force acting on piston skirt is given by [2]:

$$F_s = \tan \phi (F_G + F_{IP} + F_{IC}) \quad (11)$$

### D. Film Thickness in Hydrodynamic Regime

Considering piston eccentricities, lubricant film thickness can be approximated by [2]:

$$h = C + e_t(t) \cos x + [e_b(t) - e_t(t)] \frac{y}{L} \cos x \quad (12)$$

### E. Film Thickness in EHL Regime

By considering the bulk elastic deformation, the lubricant film thickness equation takes the following form [2]:

$$h_{ehl} = h + f(\theta, y) + v \quad (13)$$

where  $f(\theta, y)$  defines the skirts surface profile due to the

manufacturing imperfections and is neglected. The differential surface displacement is [4]

$$dv = \frac{1}{\pi E'} \frac{p(x, y) dy dy}{\dot{r}} \quad (14)$$

$$\text{where } \dot{r} = \sqrt{(x - x_0)^2 + (y - y_0)^2} \quad (15)$$

$$\frac{1}{E'} = \frac{1}{2} \left[ \frac{(1 - \nu_1^2)}{E_1} + \frac{(1 - \nu_2^2)}{E_2} \right] \quad (16)$$

At a specific point  $(x_0, y_0)$  the elastic deformation is [5]

$$v(x_0, y_0) = \frac{1}{\pi E'} \iint_A \frac{p(x, y) dx dy}{\dot{r}} \quad (17)$$

## III. NUMERICAL RESULTS AND DISCUSSION

Equation (4) defines the piston motion in the form of a pair of algebraic relationships. The forces acting and the moments generated, are shown on the right-hand side. The pair of non-linear equations constitute an initial value problem. These are solved to find out the time-based piston secondary eccentricities. Hydrodynamic film thickness is determined by solving equation (12) by guessing the values of  $e_t$ ,  $e_b$ ,  $\dot{e}_t$  and  $\dot{e}_b$  at previous time step, as initial values for the current time step. An appropriate size finite difference mesh is generated and Gauss Seidel iterative numerical scheme is employed to solve the Reynolds and the oil film thickness equations simultaneously. Then we calculate all the forces and moments in equation (4) and compute the accelerations  $\ddot{e}_t$ ,  $\ddot{e}_b$  to satisfy from the solution of velocities  $\dot{e}_t$ ,  $\dot{e}_b$  at previous and present time steps. When eccentric displacement rates  $\dot{e}_t$ ,  $\dot{e}_b$  are satisfied, the piston position at the end of the current time step is determined as [2]

$$\begin{aligned} e_t(t_i + \Delta t) &= e_t(t_i) + \Delta t \dot{e}_t(t_i) \\ e_b(t_i + \Delta t) &= e_b(t_i) + \Delta t \dot{e}_b(t_i) \end{aligned}$$

A four stroke cycle of an engine means two 360 degree crankshaft revolutions which implies  $4\pi = 720$  degree crank angle. Based on this, we define the convergence criteria of the periodic solution that is, the solution should satisfy [2]

$$\begin{aligned} e_t(t) &= e_t \left( t + \frac{4\pi}{\omega} \right); & e_b(t) &= e_b \left( t + \frac{4\pi}{\omega} \right) \\ \dot{e}_t(t) &= \dot{e}_t \left( t + \frac{4\pi}{\omega} \right); & \dot{e}_b(t) &= \dot{e}_b \left( t + \frac{4\pi}{\omega} \right) \end{aligned}$$

### A. Hydrodynamic Eccentricities and Velocities

Figure 1 shows the dimensionless piston skirts top and bottom eccentricities  $E_t$  &  $E_b$  and their profiles as a function of 720 degree crank rotation cycle. It corresponds to the four piston strokes such that 0-180 degrees, 181-360 degrees, 361-540 degrees and 541-720 degrees cover the induction, compression, expansion and the exhaust strokes, respectively. For a constant crank rotation the piston has a cyclic primary motion between the top dead centre (TDC) and the bottom dead centre (BDC). The piston has a minimum speed at respective dead centers and a maximum speed at the respective mid-strokes. The four sub-figures i.e.,

1(a), 1(b), 1(c) and 1(d) show  $E_t$  &  $E_b$  profiles curves for 10, 20, 30 and 40 microns radial clearance, respectively. In each sub-figure there are three horizontal lines. The lower line is the touching line on the major thrust side at  $-1$ , the upper line is the touching line on the minor thrust side at  $+1$  and the mid-line (zero line) indicates zero piston eccentricity. If the eccentricity curve goes beyond either the upper line or the lower line then a physical contact between the skirts and the liner surfaces gets established, inviting adhesive wear. At 10 microns clearance, piston commences its journey concentrically in the induction stroke and attains a maximum cyclic speed at the mid-stroke. At the mid-stroke it gets displaced eccentrically towards the minor thrust side and remains till the end of the induction stroke. At BDC, piston changes its direction of motion and commences its journey in the compression stroke. Such a sudden change of direction becomes the cause of an increase in the hydrodynamic film thickness. These factors cause a second eccentric displacement of the piston skirts towards the minor thrust side. After getting close to the upper line, piston stabilizes and remains at that point till it reaches at the mid-compression stroke. In the compression stroke, piston compresses the air-fuel mixture at fully closed intake and exhaust valves. It increases the magnitude of the gas pressure force, tremendously. The cumulative effects of hydrodynamic action, hydrodynamic pressures, a rising film thickness and gas force magnitude shift the secondary piston displacements towards the zero line. The piston becomes concentric with the liner as it completes the compression stroke. At that instant the air-fuel charge is fully compressed and the magnitude of the gas force is very high. Hence, despite a change in the direction of piston motion at TDC, the gas force does not allow the piston to displace eccentrically towards the minor thrust side. In the beginning of the expansion stroke combustion takes place. It causes a manifold increase in the already high magnitude of the gas pressure force. It results in a sharp eccentric displacement of the piston towards the major thrust side. Within a few degrees of piston travel after combustion, the skirts top surface comes very close to the major thrust side of the liner. However, there is no physical contact between the two interacting surfaces in relative motion during the remaining part of the expansion stroke. In the exhaust stroke, a very small magnitude of gas pressure force and very low hydrodynamic pressures fail to cause an eccentric or a concentric displacement of the piston. An increase in the radial clearance to 20 microns results in altering the eccentricity curves at particular piston positions during its travel in the four strokes. Despite a generally similar trend, the skirts top surface displaces eccentrically towards the minor thrust side in the end of the induction stroke. There is a significant change in the curve in the second half of the expansion stroke, when it goes very close to almost touch the major thrust line. At 30 microns radial clearance, improved concentric piston displacements of the skirts top and bottom surfaces occur in the expansion and exhaust strokes. At 40 microns clearance, the piston skirts displace with improved concentricity in the expansion and exhaust strokes. However, the  $E_t$  curve shifts a little further towards the minor thrust line at the end of the induction stroke. To explain such variations the corresponding secondary eccentric displacement rates or velocity profiles of the skirts top and bottom surfaces, i.e.,  $E_{t \dot{}}$  and  $E_{b \dot{}}$  are plotted, as shown in figure 2. In all the four stated clearance cases, the skirts bottom surface displaces with a high velocity

as compared to the skirts top surface. The maximum velocities of the skirts surface are at the end of the compression and exhaust strokes. Such velocities are zero in the first half of the induction stroke. Despite general similarities in the trends, the velocity magnitudes vary with the radial clearance. Such velocity variations contribute towards altering the piston eccentricities, hydrodynamic film thickness and the buildup of pressures. The maximum velocities at 10 microns clearance increase further at 20 microns clearance. However, at 30 microns clearance the magnitude of maximum velocity decreases, which helps to explain the improved concentric piston displacement in the expansion and exhaust strokes. At 40 microns clearance the maximum velocity is the lowest among all the velocities at the stated radial clearances.

### B. EHL Eccentricities and Velocities

In the EHL regime, the profile curves of eccentric piston displacements generally show a similar behavior but there are some significant differences, as shown in figure 3. At 10 microns clearance, the secondary displacement of the skirts top surface improves in the first half of the compression stroke as compared to the profile in the hydrodynamic lubrication regime. However, the skirts top surface almost comes in physical contact with the liner surface in the expansion and exhaust strokes. It was not the case in the rigid hydrodynamic lubrication regime. At 20 microns clearance, the magnitudes of the eccentric displacements do not change in the EHL regime. At 30 microns radial clearance, the eccentric piston displacements increase during the compression, expansion and exhaust strokes. Resultantly, the piston skirts top surface goes very close to the liner surface to invite the possibility of a physical contact between them. It is only at 40 microns radial clearance, when the significant improvements in the concentric piston displacements shift the skirts top surface away from the liner surface. Such a shift takes place in the compression, expansion and exhaust strokes. In the EHL regime the magnitude of the minimum hydrodynamic film thickness reduces from a few microns to a fraction of a micron. Such a reduction in the film thickness affects not only the piston eccentric displacements but also alters the magnitudes of the eccentric displacement rates or velocities. The secondary velocities at the stated radial clearances are generally higher than the corresponding velocities in the hydrodynamic lubrication regime. The respective velocity profile curves are shown in figure 4.

### C. Film Thickness in Hydrodynamic and EHL Regimes

In the hydrodynamic lubrication regime, figure 5 shows the maximum and minimum film thickness profiles i.e., *Max. Hyd. Film* and *Min. Hyd. Film*. The film thickness profile at the maximum pressure prior to the elastic deformation of the surfaces, i.e.,  $h_{pmax}$  and the film profile after the elastic deformation of the skirts and liner surfaces, i.e., *EHL Film*, are also shown. In the hydrodynamic lubrication regime, the minimum film thickness is critically important as it actually carries the hydrodynamic load. The maximum and minimum hydrodynamic film thickness profiles are different at all the four radial clearances. Despite the differences, there are some similarities in the profiles, also. The film thickness increases with the corresponding eccentric piston displacements in all the four piston strokes. Initially, a very low film thickness

results in the hydrodynamic regime due to the concentric piston motion in the first half of the induction stroke. The eccentric piston displacements enhance the buildup of hydrodynamic pressures and increase the film thickness. However, the increasing magnitudes of the piston eccentricities increase the difference in the magnitudes of the maximum and minimum film thickness in a similar proportion. At maximum values of the film thickness at the end of the compression stroke, the difference between the maximum and minimum film thickness is also maximum in all the stated radial clearances. Increasing the radial clearance from 10 microns to 40 microns increases the minimum film thickness in a similar proportion. It implies that more radial clearance is beneficial in the hydrodynamic lubrication regime. In the EHL regime, the situation is different. The EHL film thickness remains very small (a fraction of a micron) at the four stated radial clearances. The EHL film thickness profiles vary with the radial clearance. At 10 microns clearance, the EHL film rises instantaneously to a few microns in the compression stroke. It does not rise at 20 and 30 microns clearances. At 30 microns clearance, an instantaneous film thickness spike of a fairly large magnitude is not noticed in the other stated radial clearances.

*D. Hydrodynamic Pressure Rise in EHL Regime*

The pressures in the hydrodynamic lubrication regime build up gradually at varying intensities. Initially, they are biased towards the skirts top and later, towards the bottom surfaces. The different radial clearances bring some minor changes in the hydrodynamic pressure fields as the positive pressures shift from the top to the bottom surface at the end of the compression stroke. The maximum positive pressures vary and their intensities increase with the reduced radial clearance. But such changes do not occur abruptly. However, the moderate pressures buildup gradually to come close to the high values in the hydrodynamic regime. A buildup of very high pressures transforms the regime to an EHL regime. It brings some fundamental changes in the lubricant characteristics and viscosity. In the EHL regime, viscosity becomes pressure-dependent, as defined by the empirical Barus equation. The dependence of viscosity is made possible due to the tremendous increase in the hydrodynamic pressures. Such a sharp rise in the pressures increases the lubricant viscosity manifold. It causes the elastic deformation of the interacting skirts and the liner surfaces and creates an additional space to enhance the film thickness. To view the sharply rising hydrodynamic pressures in the EHL regime, the pressure fields are plotted at 10, 20, 30 and 40 microns radial clearances and shown in figure 6. In all the stated cases, the dimensionless pressures rise very high to attain the maximum values at 10 microns radial clearance. With an increase in the radial clearance, the maximum pressures rise drops proportionately to slightly reduced values. Hence, the maximum hydrodynamic pressures rise is lowest at 40 microns radial clearance. The rising EHL pressures remain in the moderate range in all the stated cases. However, starvation may increase friction and cause wear.

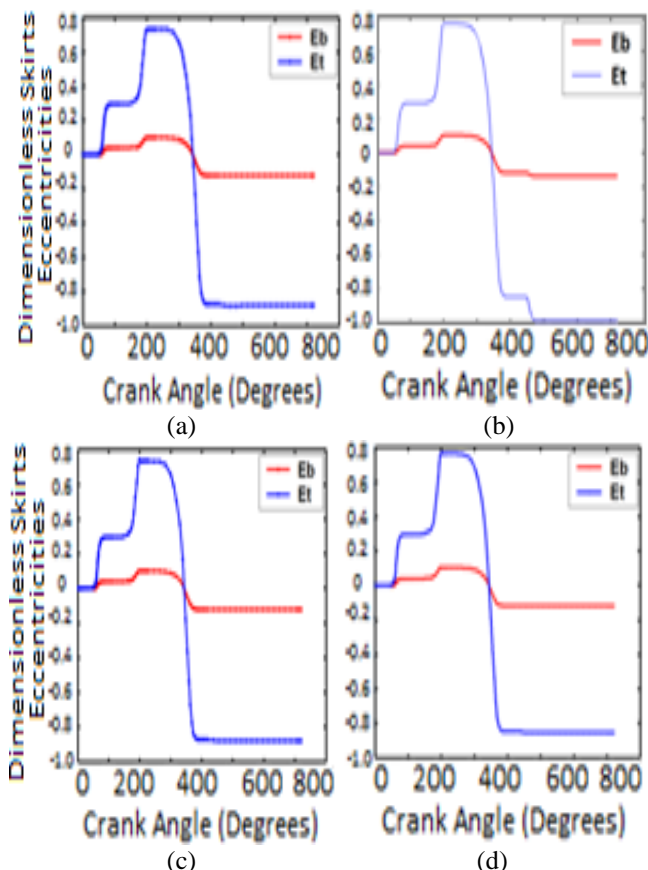


Fig:1 Dimensionless Piston Skirts Eccentricities in Hydrodynamic Regime at (a) 10 microns (b) 20 microns (c) 30 microns (d) 40 microns

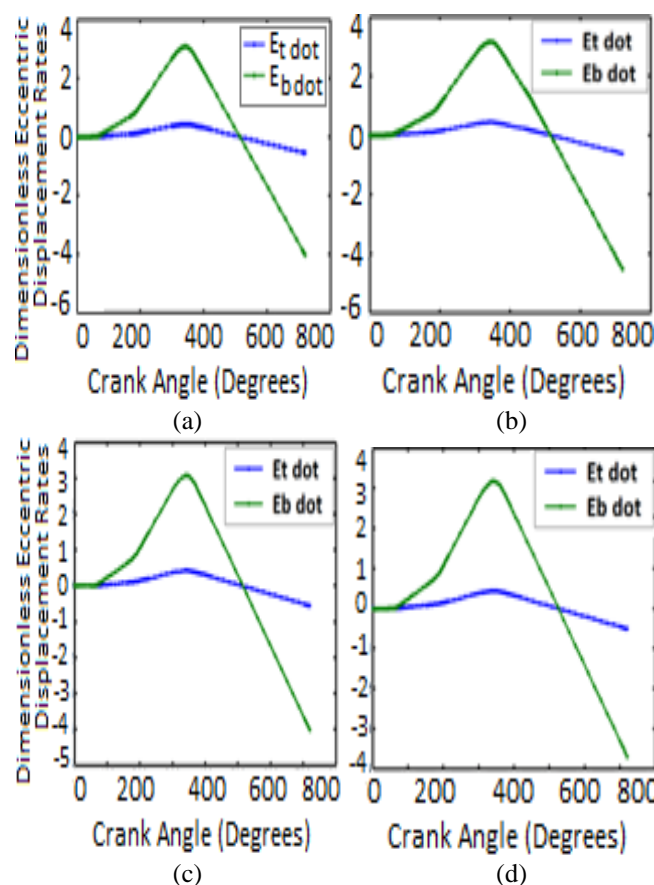


Fig: 2 Dimensionless Piston Skirts Eccentric Displacement Rates in Hydrodynamic Regime at (a) 10 microns (b) 20 microns (c) 30 microns (d) 40 microns.

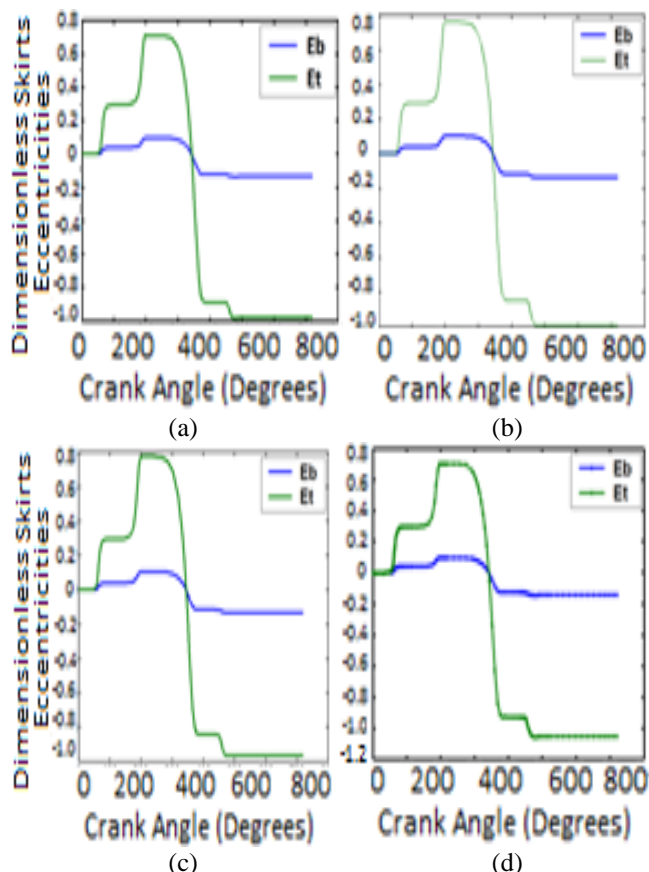


Fig:3 Dimensionless Piston Skirts Eccentricities in EHL Regime at (a) 10 microns (b) 20 microns (c) 30 microns (d) 40 microns

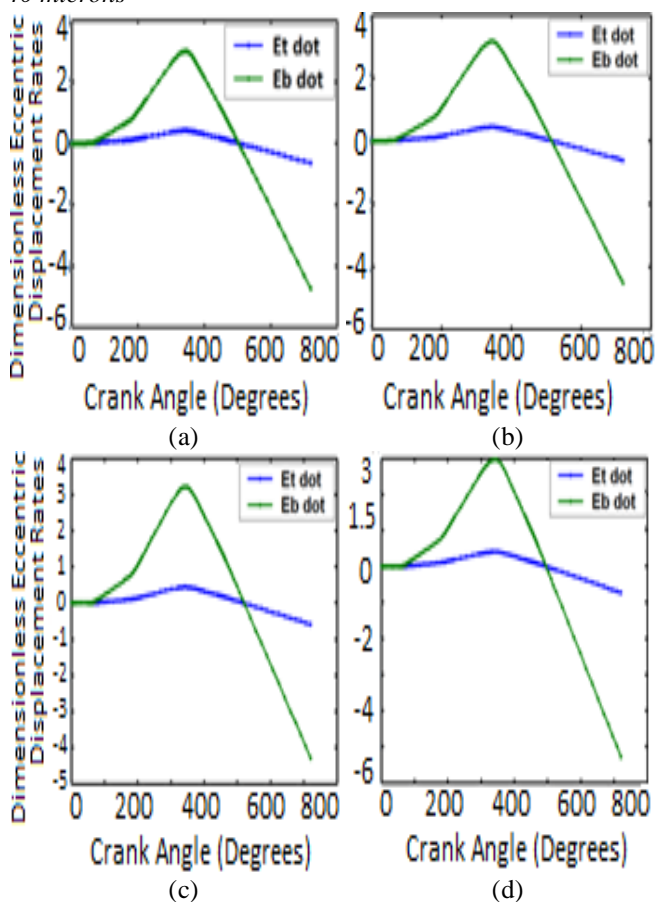


Fig: 4 Dimensionless Piston Skirts Eccentric Displacement Rates in EHL Regime at (a) 10 microns (b) 20 microns (c) 30 microns (d) 40 microns.

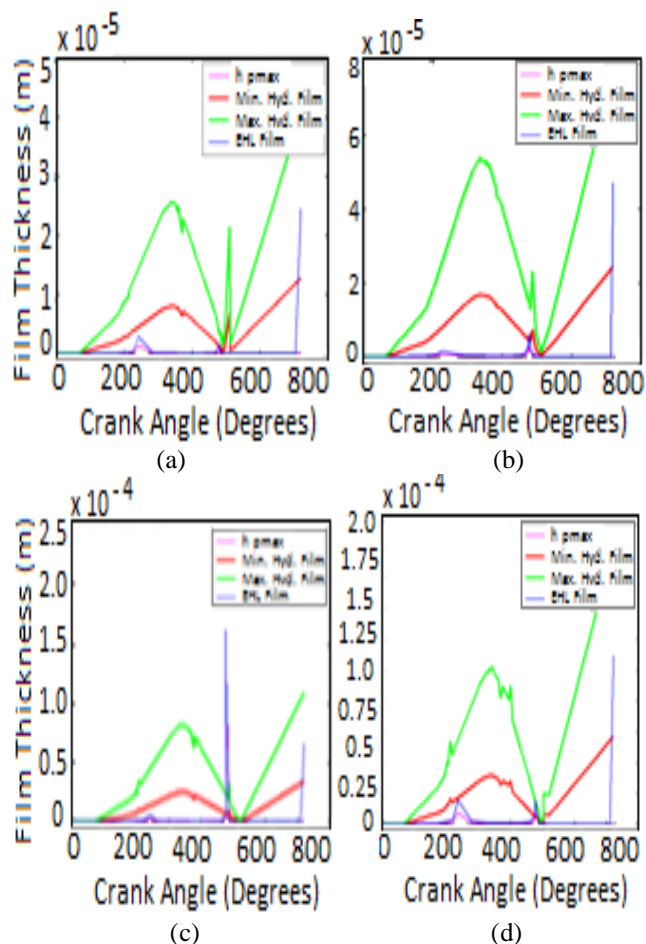


Fig: 5 Film Thickness Profiles in Hydrodynamic and EHL Regimes at (a) 10 microns (b) 20 microns (c) 30 microns (d) 40 microns.

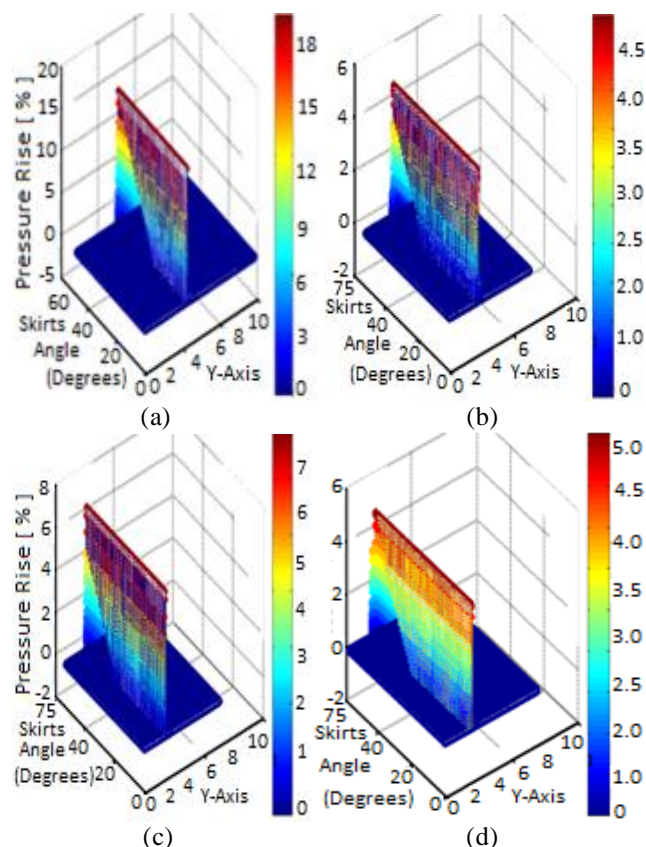


Fig: 6 Dimensionless Pressure Rise in EHL Regime at (a) 10 microns (b) 20 microns (c) 30 microns (d) 40 microns.

#### IV. CONCLUSIONS

In this paper, we have studied and investigated the effects of different small piston-to-bore radial clearances on the hydrodynamic and EHL of piston skirts. A high viscosity Newtonian lubricant was used to model the surface lubrication of piston skirts during the engine initial start up conditions. Numerical results bring some very interesting facts. A large radial clearance affects the piston's secondary displacements and modifies the transient hydrodynamic pressure and film thickness profiles. It is very significant as the small piston eccentricities decrease the chances of wear of the piston skirts in the engine start up at an idling speed. In the hydrodynamic lubrication regime, a physical contact between the skirts and the liner surfaces may conveniently be avoided at 10 microns and 40 microns clearance, respectively. However, in case of 40 microns clearance, the minimum hydrodynamic film is substantially thick than at 10 microns clearance. Hence, 40 microns clearance is the preferred optimum clearance in the rigid hydrodynamic lubrication regime at the idling engine start up speed. In the EHL regime, the situation is different. The possible solid-to-solid contact could only be avoided at 30 microns radial clearance. At this clearance, the EHL film has a thickness comparable to the other radial clearances. Moreover, the pressure does not rise very high in the EHL regime as compared to the case when the clearances are 10 and 20 microns. Hence, a radial clearance of 30 microns may be the optimum value in the EHL regime. However, further studies are needed at the other engine start up speeds using moderate and low viscosity-grade engine lubricants.

#### Nomenclature

$C$  = Piston radial clearance  
 $C_f$  = Specific heat of lubricant  
 $C_g$  = Distance from piston center of mass to piston pin  
 $C_p$  = Distance of piston-pin from axis of piston  
 $E_1, E_2$  = Young's Modulus of piston and liner  
 $F$  = Normal force acting on piston skirts  
 $F_f$  = Friction force acting on skirts surface  
 $F_{fh}$  = Friction force due to hydrodynamic lubricant film  
 $F_G$  = Combustion gas force acting on the top of piston  
 $F_h$  = Normal force due to hydrodynamic pressure in the film  
 $\widetilde{F}_{IC}$  = Transverse Inertia force due to piston mass  
 $\widetilde{F}_{IC}$  = Reciprocating Inertia force due to piston mass  
 $\widetilde{F}_{IP}$  = Transverse Inertia force due to piston-pin mass  
 $\widetilde{F}_{IP}$  = Reciprocating Inertia force due to piston-pin mass  
 $I_{pis}$  = Piston rotary inertia about its center of mass  
 $L$  = Piston skirt length  
 $M$  = Moment about piston-pin due to normal forces  
 $M_f$  = Moment about piston-pin due to friction force  
 $M_{fh}$  = Moment about piston pin due to hydrodynamic friction  
 $M_h$  = Moment about piston pin due to hydrodynamic pressure  
 $R$  = radius of piston  
 $U$  = Piston Velocity  
 $a$  = Vertical distance from piston skirt top to piston pin  
 $b$  = Vertical distance from piston skirt top to center of gravity  
 $\ddot{e}_b$  = Acceleration term of piston skirts bottom eccentricities  
 $\ddot{e}_t$  = Acceleration term of piston skirts top eccentricities  
 $l$  = Connecting rod length

$m_{pis}$  = Mass of piston  
 $m_{pin}$  = Mass of piston pin  
 $p$  = Hydrodynamic pressure  
 $r$  = Crank radius  
 $\acute{r}$  = Radius of piston  
 $u$  = Lubricant velocity component along x direction  
 $v$  = Lubricant velocity component along y direction  
 $\tau$  = Shear stress  
 $\psi$  = Crank angle  
 $\eta$  = Viscosity at ambient conditions  
 $\Phi$  = Connecting rod angle  
 $\omega$  = Crank rotation speed  
 $\nu_1, \nu_2$  = Poisson's ratio  
 $v$  = Elastic deformation of piston skirts  
 $\theta$  = Piston skirts angle in degree

#### REFERENCES

- [1] M Afzaal Malik, S. Adnan Qasim, Badar R., S. Khushnood, "Modeling and Simulation of EHL of Piston Skirts Considering Elastic Deformation in the Initial Engine Start up," Proc. 2004 ASME/STLE Int. Joint Tribol. Conf. Trib2004-64101
- [2] Dong Zhu, Herbert S. Cheng, Takayuki Arai, Kgugo Hamai, "A Numerical Analysis for Piston Skirts in Mixed Lubrication," ASME. 91-Trib-66.
- [3] Gwidon W. Stachowiak and Andrew W. Batchelor, (Book) *Engineering Tribol*, 3rd Ed., Elsevier; pp. 112-219 I
- [4] Dowson D., Higginson G.R., Book, "Elasto-Hydrodynamic Lubrication: The Fundamentals of Gear And Roller Lubrication", 1966, pp 55-106.
- [5] Iya I. Kudish, Rubber G. Airapetyan and Michael J. Covitch, "Modeling of Lubricant Degradation And EHL," IUTAM Symposium on EHD and Micro EHDs, 1<sup>st</sup> ed. 149-1, 2006, Springer.
- [6] Ming-Tang Ma, "An Expedient Approach to the Non-Newtonian Thermal EHL in Heavily Loaded Point Contacts," *Wear* 206 (1997) 100-112.
- [7] Hong Yiping, Chen Darong, Kong Xianmei, Wang Jiadao, "Model of Fluid Structure Interaction and Its Application to EHL," *Computer Methods Application in Mechanical Engineering*, 191.(2002). 4231-4240.
- [8] J. P. Charmleffel, G. Dalmaz, P.Vergne, "Experimental Results and Analytical Film Thickness Predictions in EHD Rolling Point Contacts," *Tribol. International*, 40 (2007) 1543-1552.
- [9] J. G. Wang and J. J. Ma, "On the Shear Stress of Elastohydrodynamic Lubrication in Elliptical Contacts," *Tribol. International*, Vol. 29. 0301-679x(96)0005-9.
- [10] Sara J .Hupp, "Defining The Role of Elastic Lubricants and Micro Textured Surfaces In Lubricated, Sliding Friction" PhD Thesis , Massachusetts Institute of Technology, Feb 2008.